

Effect of Fe doping on TiO₂ films prepared by spin coating

C.Y.W. Lin, D. Channei, P. Koshy, A. Nakaruk^{*}, C.C. Sorrell^{*}

School of Materials Science and Engineering, University of New South Wales, Sydney, NSW 2052, Australia

Received 21 December 2011; accepted 15 January 2012

Available online 25 January 2012

Abstract

Iron-doped titanium dioxide thin films were coated on fluorine-doped tin oxide coated glass using the spin coating technique. The concentration of the dopant was varied up to 7 mol% iron (metal base). The films were characterised for their structural, morphological, and optical properties. Glancing angle X-ray diffraction and laser Raman microspectroscopy indicate that the films consisted solely of the anatase polymorph of titanium dioxide, without any contamination phases, such as iron oxide. Field emission scanning electron microscopy indicates that the films were microstructurally homogeneous and fully dense, with grains in the size range of ~10–20 nm. UV-VIS spectrophotometry shows that the optical indirect band gap of the films decreased with increasing iron doping (3.36 eV for undoped and 2.95 eV for 7 mol% Fe).

© 2012 Elsevier Ltd and Techna Group S.r.l. All rights reserved.

Keywords: Titanium dioxide; Fe doping; Spin coating; X-ray photoelectron spectroscopy

1. Introduction

Over the last few decades, titanium dioxide (TiO₂, titania) has been investigated extensively for a range of applications owing to a number of advantages, which include long-term environmental stability, nil toxicity, inertness to acids, and significant photocatalytic behaviour [1]. Furthermore, TiO₂ has been found to be the most suitable material for a wide range of environmentally beneficial applications, including water and air purification [2,3]. However, TiO₂ is a wide band gap ($E_g = 3.2$ eV) semiconductor [4], and so it can absorb only in the ultraviolet (UV) region of sunlight; this indicates that only ~5% of incident sunlight can be absorbed [4]. Therefore, in order to improve the photocatalytic activity of TiO₂ in the visible region, modification of the band gap by doping with transition metals, including Cr [5], Mn [4], Fe [6], and Zn [7], has been studied. Of the preceding dopants, Fe has attracted strong interest owing to its octahedral trivalent radius of 0.079 nm, which is similar to that of octahedral tetravalent Ti (0.075 nm) [8]. Therefore, it can be inferred that Fe³⁺ ions can be incorporated in the Ti⁴⁺ sublattice of TiO₂, which also could

enhance oxygen vacancy formation, potentially leading to an improvement in the photocatalytic performance [9].

Fe-doped TiO₂ thin films can be prepared by several techniques, including sputtering [10], metal organic chemical vapour deposition (MOCVD) [11], dip coating [12], ultrasonic spray pyrolysis [13], and spin coating [14]. The latter is considered as one of the most advantageous techniques due to its effectiveness, versatility, and practicality. Importantly, it does not require a vacuum system since the process can be carried out at atmospheric conditions.

In the present work, Fe-doped TiO₂ films were deposited on F-doped SnO₂-coated glass (FTO-coated) using spin coating. The effect of the dopant concentration was investigated in terms of the structural, morphological, and optical properties of the resultant thin films.

2. Methodology

Solution precursors were prepared using Ti isopropoxide (TIP, Reagent Grade, 97 wt.%, Sigma–Aldrich) dissolved in isopropanol (Reagent Plus, ≥99 wt.%, Sigma–Aldrich) at a Ti concentration of 0.1 M (2.8 g of TIP diluted to 100 mL volume with isopropanol); the solutions were mixed by stirring in a Pyrex beaker at 400 rpm with a Teflon-coated rod for 10 min without heating. The Fe dopant concentration was varied to 1, 3, 5, and 7 wt.% Fe (metal basis relative to Ti isopropoxide) by

^{*} Corresponding authors. Tel.: +61 2 9385 4421; fax: +61 2 0395 5956.

E-mail addresses: A.Nakaruk@unsw.edu.au (A. Nakaruk),
C.Sorrell@unsw.edu.au (C.C. Sorrell).

adding FeCl_3 (Reagent Plus, ≥ 99 wt.%, Sigma–Aldrich) to the solution with hand stirring. The Fe was added on the basis of stoichiometric TiO_2 ; that is, there was no compensatory decrease in the Ti levels. Spin coating (Laurell WS-65052) was done by rapidly depositing ~ 0.2 mL (ten sequential drops) of solution onto an FTO-coated glass substrate (WuHan Geao Instruments Science & Technology Co., Ltd., China) spun at 2000 rpm in air. The film was dried by spinning for an additional 15 s. This process was repeated four more times (*viz.*, ~ 1 mL; fifty drops) in order to obtain as-deposited thin films of ~ 500 nm thickness. Subsequent annealing was done in a muffle furnace at 500°C with a heating rate of $5^\circ\text{C}/\text{min}$ and soak time of 5 h, followed by natural cooling.

The mineralogies of the films were determined by glancing angle X-ray diffraction (GAXRD, Phillips *X'pert Materials Research Diffraction*, $\text{CuK}\alpha$, 45 kV, 40 mA, step size $0.02^\circ 2\theta$ speed $6^\circ/\text{min } 2\theta$) and laser Raman microscopy (He–Cd UV laser excitation source of wavelength 442 nm, Renishaw *inVia*). Field emission scanning electron microscopy (FESEM, Nova *NanoSEM 230*; Cr-coated, secondary electron emission mode, 2 kV accelerating voltage) was used to investigate the morphologies of the films. The chemical compositions and metal valences were investigated using X-ray photoelectron spectroscopy (XPS, Thermo Scientific, *ESCALAB250Xi*). The transmission in the ultraviolet-visible (UV-VIS) range was determined using a dual-beam spectrophotometer (Perkin Elmer *Lambda 35*); the optical indirect band gap was calculated from these data using the method of Tauc and Menth [15].

3. Results and discussion

The GAXRD patterns, given in Fig. 1, show that, with increasing Fe dopant levels, the anatase peaks become broader and smaller, which suggests decreasing degree of crystallinity. Further, the laser Raman microspectra (data not shown) tend to confirm the GAXRD results in that they also show a decrease in

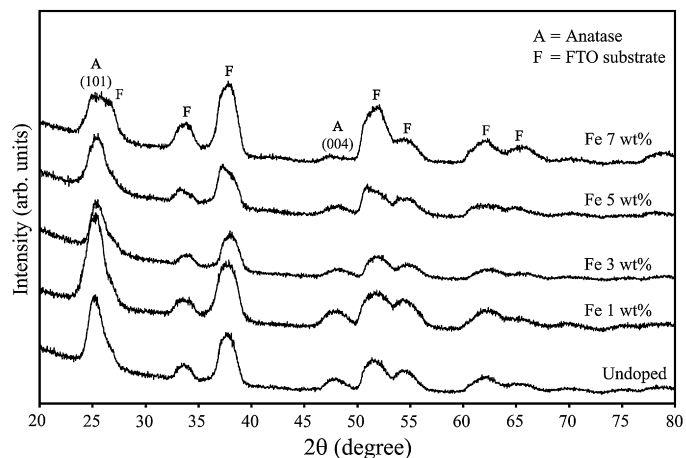


Fig. 1. Glancing angle X-ray diffraction data of Fe-Doped TiO_2 Films.

anatase peak intensities with increasing Fe dopant levels. Since the Fe was added to stoichiometric TiO_2 , it is clear that the accommodation of the former in the lattice, whether substitutional or interstitial, results in structural distortion and concomitant decrease in crystallinity [9].

Fig. 2 shows FESEM images of the films containing the different Fe dopant levels. These data show that the films are microstructurally homogenous, with no pinholes, and the grains were in the size range of ~ 10 – 20 nm. It is clear that Fe^{3+} had no effect on enhancing the grain growth that accompanies the anatase \rightarrow rutile phase transformation, which generally is considered to occur at temperatures $\geq 600^\circ\text{C}$, although it can occur $< 500^\circ\text{C}$ [9].

Table 1 shows the results of the XPS measurements, which reveal that contamination of the film by the substrate occurred. It should be noted that Fe^{3+} , Sn^{4+} , and Na^{1+} are known to enhance the anatase \rightarrow rutile phase transformation [9] while Si^{4+} is known to suppress it.

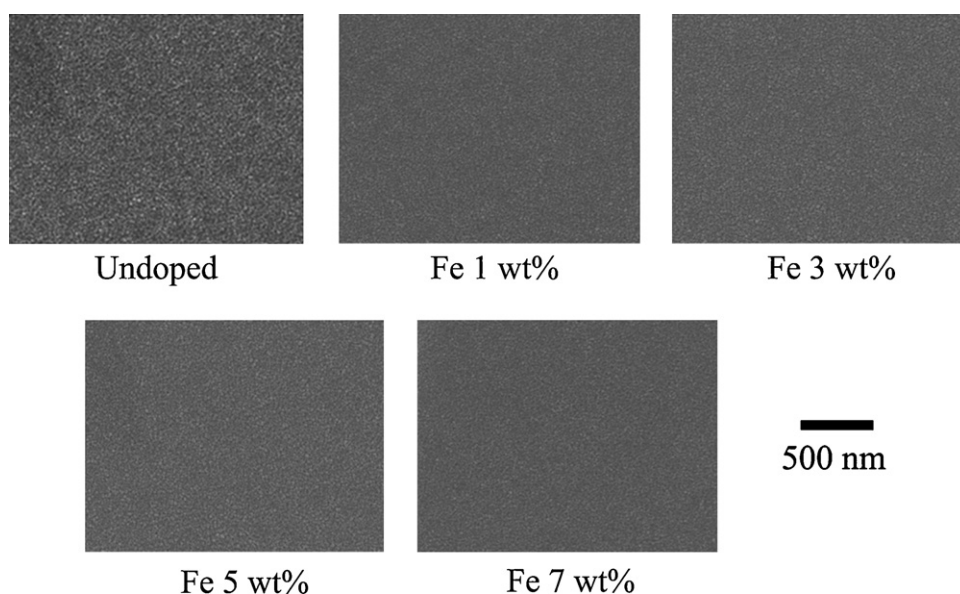


Fig. 2. Field emission scanning electron microscopy images of Fe-Doped TiO_2 Films.

Table 1
Summary of analytical data.

Fe dopant level added (wt.%)	Dopant/contaminant level determined by XPS (wt.%)				Transparency (%)	Optical indirect band gap (eV)
	Fe ³⁺	Sn ⁴⁺	Si ⁴⁺	Na ¹⁺		
0	0.00	1.15	1.37	1.56	70–80	3.36
1	0.54	1.15	0.00	1.29		3.24
3	1.82	1.88	0.00	1.51		3.13
5	3.01	1.41	0.00	1.83		3.04
7	5.57	1.70	0.00	1.46		2.95

Since Si⁴⁺ was detected only in the undoped film, while Fe³⁺, Sn⁴⁺, and Na¹⁺ were detected in all doped films, the retention of anatase might be expected. It is likely that the annealing conditions of 5 h at 500 °C were insufficient to cause the phase transformation.

The XPS data also reveal other features:

- The Fe³⁺ levels were lower than added initially. This probably is a result of the diffusion of this ion into the substrate. Diffusion of Fe²⁺ and Fe³⁺ into fused silica glass at only 400 °C has been reported before [16].
- The films were contaminated by Sn⁴⁺ owing to diffusion from the FTO coating on the substrate. The absence of a trend indicates that this is a relatively consistent effect, unaffected by the Fe dopant level.
- The films also were contaminated by relatively consistent levels of Na¹⁺ owing to diffusion from the soda-lime–silica substrate. The diffusion of the small and mobile Na¹⁺ ion is well known.
- Contamination of the undoped film only by Si⁴⁺ is notable. Since Fe³⁺ is absent in the undoped film and Sn⁴⁺ is present, this observation suggests Sn⁴⁺ is not causative and that counter-diffusion and/or blocking of Ti⁴⁺ lattice sites by Fe³⁺ may be responsible for suppression of Si⁴⁺ diffusion and resultant contamination of the doped films.

The UV–VIS spectra of the films are shown in Fig. 3. It can be seen that, in both the UV (≤ 400 nm) and visible (400–800 nm) regions, the transmission generally decreased with increasing Fe dopant levels. Further, the absorption edge shifted to longer wavelengths with increasing Fe dopant levels, thereby increasing the radiation absorption. The presence of interference fringes in the transmission spectra indicates that the films

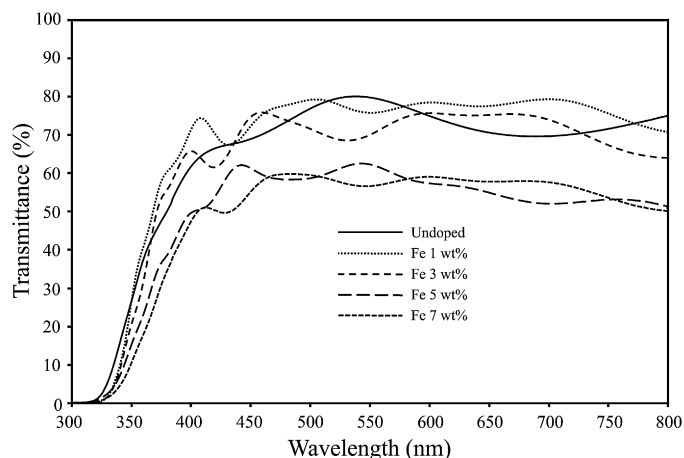


Fig. 3. UV–VIS spectra data of Fe-Doped TiO₂ Films.

are smooth and microstructurally homogenous [17]. These data confirm the observations of the FESEM analyses.

The optical indirect band gap of films can be calculated from UV–VIS spectrophotometry data, the details of which are described elsewhere [13,15,18]. The values obtained from these data are listed in Table 1.

Fe³⁺ is known to create shallow trapping sites at the donor and acceptor levels [19], as shown in Fig. 4 (left). This effective decrease in the band gap means Fe-doped films can absorb more light in the visible region than undoped films, thereby increasing the efficiency of the photocatalytic performance of the material.

The calculated thermodynamic stability diagram of Fe–O, as given in Fig. 4 (right), shows that the annealing conditions of 500 °C in air result in the existence of Fe³⁺ only. The XPS data

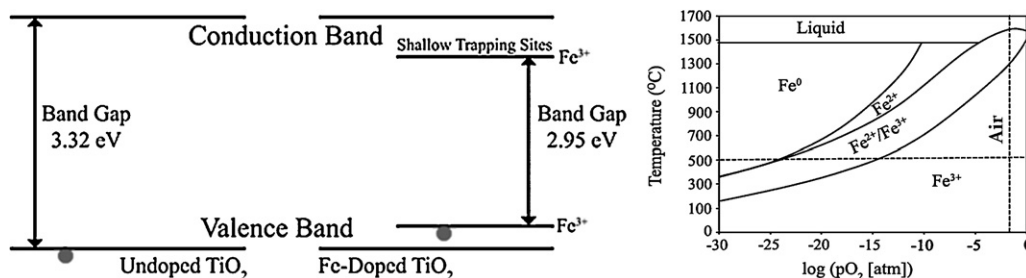


Fig. 4. Hypothetical band structure of Fe-doped TiO₂ (left) and thermodynamic stability diagram for Fe–O (right).

confirm this, showing only Fe^{3+} and the absence of other ions, such as Fe^{2+} and Fe^{4+} , which is common with previous studies [20,21].

4. Summary and conclusions

Fe-doped TiO_2 thin films coated on FTO substrates using spin coating have been produced. The thin films were reproducible and high quality, as shown by the consistent bulk densities, thicknesses, grain sizes, surface profiles, UV–VIS spectra, and dopant retention of all of the thin films. The GAXRD and laser Raman microspectroscopy analyses show that the films consisted of anatase only, with no formation of secondary phases, such as Fe_2O_3 . Further, these results indicate that the presence of incorporated Fe results in lattice distortion. The FESEM images show that the grain size of the films was consistent and in the range ~ 10 – 20 nm. The UV–VIS data show that the films were relatively transparent and had smooth surfaces. Increasing Fe dopant levels caused a significant decrease in the optical indirect band gap. The contamination of the films by Sn^{4+} , Na^{1+} , and/or Si^{4+} is an important variable that requires further investigation. The effect of Si^{4+} is particularly important because thin films deposited on quartz and glass following by annealing for recrystallisation, which is the vast majority, are subject to what is likely to be a near-universal contaminant.

Acknowledgements

The authors would like to acknowledge financial support from the Australian Research Council and the UNSW node of the Australian Microscopy & Microanalysis Research Facility (AMMRF).

References

- [1] T. Bak, J. Nowotny, M. Rekas, C.C. Sorrell, Photo-electrochemical hydrogen generation from water using solar energy. Materials-related aspects, *Int. J. Hydrogen Energy* 27 (2002) 991–1022.
- [2] R. Wang, K. Hashimoto, A. Fujishima, M. Chikuni, E. Kojima, A. Kitamura, M. Shimohigoshi, T. Watanabe, Photogeneration of highly amphiphilic TiO_2 surfaces, *Adv. Mater.* 10 (1998) 135–138.
- [3] I.P. Parkin, R.G. Palgrave, Self-cleaning coatings, *J. Mater. Chem.* 15 (2005) 1689–1695.
- [4] Q.R. Deng, X.H. Xia, M.L. Gua, Y. Gao, G. Shao, Mn-doped TiO_2 nanopowders with remarkable visible light photocatalytic activity, *Mater. Lett.* 65 (2011) 2051–2054.
- [5] G.H. Takaoka, T. Nose, M. Kawashita, Photocatalytic properties of Cr-doped TiO_2 films prepared by oxygen cluster ion beam assisted deposition, *Vacuum* 83 (2009) 679–682.
- [6] M.C. Wang, H.J. Lin, T.S. Yang, Characteristics and optical properties of iron ion (Fe^{3+})-doped titanium oxide thin films prepared by a sol–gel spin coating, *J. Alloy Compd.* 473 (2009) 394–400.
- [7] L. Jing, B. Xin, F. Yuan, L. Xue, B. Wang, H. Fu, Effects of surface oxygen vacancies on photophysical and photochemical processes of Zn-Doped TiO_2 nanoparticles and their relationships, *J. Phys. Chem. B* 110 (2006) 17860–17865.
- [8] R.D. Shannon, Revised effective ionic radii and systematic studies of interatomic distances in halides and chalcogenides, *Acta Crystallogr. A* 32 (1976) 751–767.
- [9] D.A.H. Hanaor, C.C. Sorrell, Review of the anatase to rutile phase transformation, *J. Mater. Sci.* 46 (2011) 855–874.
- [10] M.F. Hossain, S. Biswas, T. Takahashi, Y. Kubota, A. Fujishima, Investigation of sputter-deposited TiO_2 thin film for the fabrication of dye-sensitized solar cells, *Thin Solid Films* 516 (2008) 7149–7154.
- [11] N. Baguer, E. Neyts, S. Van Gils, A. Bogaerts, Study of atmospheric MOCVD of TiO_2 thin films by means of computational fluid dynamics simulations, *Chem. Vapor Depos.* 14 (2008) 339–346.
- [12] D.J. Kim, S.H. Hahn, S.H. Oh, E.J. Kim, Influence of calcination temperature on structural and optical properties of TiO_2 thin films prepared by sol–gel dip coating, *Mater. Lett.* 57 (2002) 355–360.
- [13] A. Nakaruk, D. Ragazzon, C.C. Sorrell, Anatase–rutile transformation through high-temperature annealing of titania films produced by ultrasonic spray pyrolysis, *Thin Solid Films* 518 (2010) 3735–3742.
- [14] A. Nakaruk, C.Y. Lin, D.S. Perera, C.C. Sorrell, Effect of annealing temperature on titania films prepared by spin-coating, *J. Sol-gel Sci. Technol.* 55 (2010) 328–334.
- [15] J. Tauc, A. Menth, States in the gap, *J. Non-Cryst. Solids* 8–10 (1972) 569.
- [16] P.W. Wang, Y.P. Feng, W.L. Roth, J.W. Corbett, Diffusion behavior of implanted iron in fused silica glass, *J. Non-Cryst. Solids* 104 (1988) 81–84.
- [17] R. Swanepoel, Determination of surface roughness and optical constants of inhomogeneous amorphous silicon films, *J. Phys. E* 17 (1984) 896.
- [18] D. Mardare, M. Tasca, M. Delibas, G.I. Rusu, On the structural properties and optical transmittance of TiO_2 r.f. sputtered thin films, *Appl. Surf. Sci.* 156 (2000) 200–206.
- [19] J. Nowotny, C.C. Sorrell, L.R. Sheppard, T. Bak, Solar-hydrogen: environmentally safe fuel for the future, *Int. J. Hydrogen Energy* 30 (2005) 521–544.
- [20] H. Zhang, H. Liu, C. Mu, C. Qiu, D. Wu, Antibacterial properties of nanometer Fe^{3+} - TiO_2 thin films, in: *Proceeding of the 1st IEEE International Conference on Nano/Micro Engineered and Molecular System*, China, (2006), pp. 955–958.
- [21] J. Ma, Y. Wei, W.X. Liu, W.B. Cao, Separation of nanocrystalline Fe-doped TiO_2 powders as a visible-light-responsive photocatalyst, *Res. Chem. Intermed.* 25 (2009) 329–336.